

Kinetics of Nucleation from Aqueous Solution

Homogeneous nucleation is achieved in aqueous systems by creating adequately high levels of supersaturations. This process can be fully described by considering depletion of supersaturation due to simultaneous growth of the nuclei. Nielsen (1964) formulated this by integrating the growth kinetics with classical nucleation theory. This paper uses his combined nucleation-growth approach, as well as more recently developed mechanisms of adding monomers to developing nuclei (Chiang et al., 1988). The experimental data considered suggest that the systems fall into two categories: one involving the same mechanism for nucleation and growth and the other involving different mechanisms. A dimensionless parameter which evolves in the development permits the comparison of the rate of nuclei formation with that of nuclei growth. The inferences from this approach suggest further that the surface energy parameter is an indicator of the category to which a solution system belongs.

Rita Mohanty
Suhas Bhandarkar
Joseph Estrin

Department of Chemical Engineering
University of Rhode Island
Kingston, RI 02881

Introduction

As a basic phenomenon of phase change, homogeneous nucleation in pure vapor systems is well understood. Vapor-liquid nucleation theory has been supported by the results of the superbly devised experiments which permit careful probing into the basics of the phenomenon. These include expansion cloud chamber (Schmitt, 1988), diffusion cloud chamber (Katz, 1970), and supersonic nozzle (Wegener, 1975) methods. Even for these systems, controversy exists concerning the more refined details of the theory (Lothe and Pound, 1962). Although many of the same first principles are still applicable when considering homogeneous nucleation from condensed-phase solution, the same level of understanding is not in hand. Corresponding theoretical and experimental methods are not available.

The primary thrust of this paper is based on the experimental method of Nielsen (1964, 1969). He employed a rapid mixing device in which two reactive solutions were introduced into each other, and the time of first visual occurrence of precipitate and the number of precipitate entities formed were measured. These were determined over a range of supersaturations which were assumed to exist momentarily after complete fluid mechanical mixing. Nielsen's modeling of the process assumes nucleation

from a fully mixed or homogeneous solution: $t_m < t_i$ where t_m is the characteristic mixing time and t_i is the measured induction time assumed to represent the characteristic reaction kinetic time. Nuclei formation reaction occurs as described by classical theory which, in particular, calls upon Brownian motion for description of the kinetics part of the model. Nielsen considered the total number of nuclei formed N to be determined by simultaneous occurrence of nucleation and growth. He accounted for depletion of supersaturation by growth which determines the termination of nucleation as it is more sensitive to the level of supersaturation. The number measured and the number predicted by the model refer to the same dependent variable N .

It is important to point out concerning the experimental method that the occurrence of homogeneous nucleation is assured because the numbers observed are much greater than that of heteronuclei typically present in aqueous media. That is, the uncertainties which exist because of the unavoidability of heterogeneous nucleation are bypassed by providing that N (experimental) $\approx N$ (homogeneous origin) $\gg N$ (heterogeneous origin) (Nielsen, 1964). Nielsen's simplified modeling procedure is employed in the following discussion. It emphasizes the salient steps which describe the phenomenon. The departure from his model occurs here in the realization that the rate-controlling kinetics of nucleation are not determined solely by

Correspondence concerning this paper should be addressed to J. Estrin.

Brownian or molecular diffusion mechanics. Recently, Narsimhan and Ruckenstein (1989) have shown how Brownian motion kinetics are incorporated into the model so that little emphasis is required of strictly thermodynamic arguments. Chiang et al. (1988) have elaborated on the nucleation process from solutions of ionic solute. They employed nucleation and growth kinetics intimately in elucidating their kinetics-based models for nucleation. Their analysis is developed within the kinetic-thermodynamic structure provided by Katz and Donohue (1979), and thereby retains more rigor than is found in typical classical presentations. Nielsen's modeling lacks the rigor of these recent papers but it clearly considers the topics of significance. By associating the primary kinetics of nucleation and growth in examining several kinetics schemes, we have introduced the points made by Chiang et al. (1988) into Nielsen's model. This helped us understand the relationships among the several concepts involved because they result in simpler formulae.

Classical Theory

Figure 1 shows the general ideas behind Nielsen's model. Curves N represent a number of nuclei which are products of the nucleation process up to time t_1 , i.e., $N(t/t_1)$. The curves c represent the concentration, $c(t/t_1)$, and J the nucleation rate per unit volume of homogeneous solution, $J(t/t_1)$. The dotted curves were derived on the basis of Nielsen's simplified approximate modeling. The simplified concentration profile leads to a characteristic time t_1 at which point $c = c_c$. The coincidence of the two curves c , dotted and full, for a small time is adequate to cover approximately the period over which $J > 0$ because of the strongly exponential dependence of J upon c . The characteristic time t_1 then estimates the period during which nucleation decays completely. It therefore approximates the induction time t_i (time of first appearance of precipitate) and serves as a scaling factor by which both $J(t/t_1)$ and $c(t/t_1)$ are estimated to allow direct integration of the equation

$$N \int_0^{t_1} J dt. \quad (1)$$

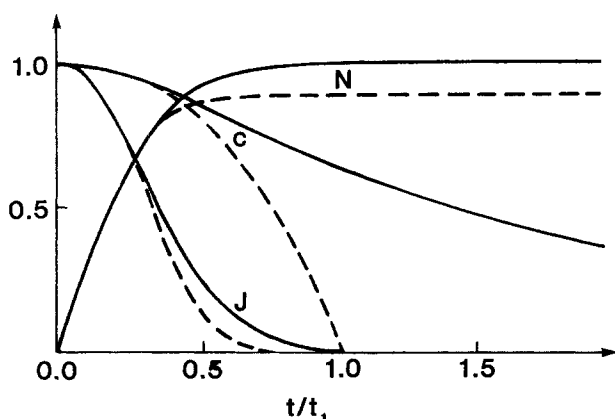


Figure 1. Normalized profiles of c , J and N plotted as a function of time t , scaled with respect to the induction period t_1 .

The full curves correspond to the full-blown theory, using c as in Eq. 5A; the broken curves result from the approximate expression for c given by Eq. 8A (after Nielsen, 1969).

The usefulness of the analysis giving closed form estimates rests on the fact that both N and t_1 may be experimentally obtained. Tacit in the above are the requirements

$$t_n < t_i \approx t_1,$$

where t_n is the time required for the establishment of the steady-state nucleation kinetics (Chiang et al., 1988; Narsimhan and Ruckenstein, 1989).

In describing the homogeneous nucleation from solution, we involve only ion groups or molecules or formula units such that c is the mean concentration (Nielsen, 1969), that is, the concentration of solute molecules. There is no ambiguity when the solution is composed of reactants in stoichiometric proportions as used throughout this work. For nonstoichiometric proportions, extension of the meaning of c has been discussed elsewhere in the recent literature (Chiang and Donohue, 1988b). The expression for the free energy of formation of a crystalline cluster of n units is modeled as: a) the free energy change associated with incorporating n formula units of ions from supersaturated solution into a bulk crystal of the product in equilibrium with saturated solution at the current temperature and pressure of the solution; and b) as the excess free energy representing the crystal-solution interface of a solute nucleus of size n . The free energy of formation of such an n -size unit is then

$$\Delta G(n) = -nkT \ln S + \sigma A(n) \quad (2)$$

where S is the supersaturation ratio, c/c_c , σ is the interfacial energy, and A is the area of the interface and is determined by the number of units making up the nucleus. By defining a generalized radius

$$r = 3V/A$$

where V is the volume of the nucleus, whose results at critical size

$$r^* = 2\sigma v/kT \ln S \quad (3)$$

$$n^* = V^*/v = 2\beta\sigma^3 v^2/(kT \ln S)^3 \quad (4)$$

where β is a geometric factor introduced by Nielsen to account for other geometries, e.g., $\beta = 32$ for cubes and $16\pi/3$ for spheres. The maximum value of ΔG is for a given supersaturation,

$$\Delta G^* = \beta\sigma^3 v^2/(kT \ln S)^2 \quad (5)$$

This represents the energy barrier which must be overcome before a nucleus may grow spontaneously: for $n < n^*$ the typical entity dissolves, for $n > n^*$ it grows because of favorable (adequately superaturated) surroundings.

The modification of the Zeldovich (1943) and Frenkel (1955) developments by Kagan (1960) is employed here. It clarifies some points of the results from Nielsen-type experiments. The assumption that the formation of a steady-state distribution of embryonic species is made at the outset. It is designated by the density function f_n which has the significance that the number of embryonic entities between sizes n_1 and n_2 , per unit volume, may

be expressed as

$$\int_{n_1}^{n_2} f_n dn$$

The flux of embryos or nuclei past any size n is given by

$$J_n = \dot{n}f_n - D_n df_n/dn, \quad (6)$$

where \dot{n} is the mean growth rate of an entity of size n as the net number of molecules added to the embryo or nucleus per unit time, and D_n is the function which permits relating a contribution to the flux due to the gradient in f_n . This population balance is justified only heuristically and differs from that developed by Narsimhan and Ruckenstein in that D_n is not justified through explicit consideration of addition-departure kinetics. Rather, D_n is a function of n yet to be determined.

Since the steady state has been assumed, there is no accumulation of clusters and J_n is independent of n and must be equal to the rate of nucleation J . Therefore, it is assumed that when no nucleation occurs ($J = 0$), the distribution f_n and the function D_n retain their significance. The former is given by the Boltzmann distribution

$$f_{n0} = N_o \exp [-\Delta G(n)/kT], \quad (7)$$

where f_{n0} represents f_n when $J \rightarrow 0$ exists and the latter

$$D_n = \dot{n}/(d \ln f_{n0}/dn) = -\dot{n}kT/(d\Delta G/dn) \quad (8)$$

There is a lack of rigor in these steps due to the implied assumption of "constrained equilibrium" (Katz and Donohue, 1979): despite the existence of adequate supersaturation such that $J > 0$, the formulation of D_n as given in Eq. 8 is taken to be correct. Because of the complexities in condensed-phase solution system processes, this seems justified for practical reasons. This approach is supported by the observation that the righthand formula for D_n above depends explicitly on the growth rate \dot{n} and the "driving force" for crystal growth $d\Delta G/dn$. The size distribution of embryos f_n is not involved conceptually in either case.

Making use of Eq. 8 and the boundary condition

$$f_n \rightarrow 0 \quad \text{as} \quad n \rightarrow \infty$$

the solution to the differential Eq. 6 is obtained (Kagan, 1960) on requiring that $f_n \approx f_{n0}$ when $r \ll r^*$, say when $r \rightarrow 0$,

$$f_n = J \exp [-\Delta G(n)/kT] \int_n^\infty (1/D_r) \exp [\Delta G(r)/kT] dr \quad (9)$$

and when $r \rightarrow 0$ and it is rearranged

$$J = N_o \left(\int_0^\infty (1/D_r) (dn/dr) \exp [\Delta G(r)/kT] dr \right)^{-1} \quad (10)$$

Generally the exponential in the integrand is so peaked that the integral is dominated by its value at $r = r^*$. Therefore, the preexponential factors in the integrand, evaluated at r^* , may be

removed, and Eq. 10 rewritten

$$J = N_o D_r^* (dr/dn)^* / \left(\int_0^\infty \exp [\Delta G(r)/kT] dr \right). \quad (11)$$

The superscript $*$ indicates evaluation at r^* . As long as the mechanism is reversible, we may call upon the Kelvin effect, i.e., the entity size—solubility relationship, to describe that $(dr/dt)^* = 0$. The Kelvin equation may be written

$$c - c_e \exp [\Gamma/r] = 0 \quad (12)$$

where $\Gamma = 2\sigma v/kT$. From Eqs. 2 and 3 and the spherical geometry assumption

$$(d^2\Delta G/dr^2)^* = -8\pi\sigma \quad (13)$$

Elaboration of eligible growth rate expressions for (dr/dt) are required to complete discussion of the preexponential factor in the nucleation expression. As the driving force for growth is zero at $r = r^*$ were required that D_r from Eq. 8 be evaluated through use of L'Hospital rule. The integral in Eq. 11 may be evaluated by expanding r^* to obtain (Kagan, 1960; Strickland-Constable, 1968), after making use of Eqs. 3, 4, 5 and 8,

$$J = N_o (kT/\sigma)^{1/2} (r^{*2}/v) [(d(dr/dt)/dr)^*] \cdot \exp [-\Delta G^*/kT] \quad (14)$$

For gaseous systems, the preexponential factor involves use of gas theory to provide the rate at which solute gaseous molecules impinge on the embryonic surface (Katz and Donohue, 1979). For condensed systems, most typically Brownian motions or equivalent (Narsimhan and Ruckenstein, 1989) provide a mechanism for the impingement rate noted above. On this basis, the equation Nielsen derived for water-like dilute solutions is

$$J = 2Dd^{-5} \exp [-\Delta G^*/kT] \quad (15)$$

where d is the molecular diameter (Nielsen, 1964). He described this as being acceptable to about a factor of 10. Implied in Brownian-based impingements is the assumption that no interface kinetics contributes to rate control. (In gas theory use is made of a condensation coefficient ≤ 1 to take into consideration that each impingement may not lead to a successful incorporation into the matrix of the embryonic entity.)

Chiang and Donohue (1988a) studied crystallization growth kinetics from ionic solution and extended this (Chiang et al., 1988) to include nucleation kinetics as developed by Katz and Donohue (1979). Their work is of fundamental importance, and reference to it will be made in the development of Nielsen's work here. Specifically, a basic concept involved is that the nucleation kinetics and growth kinetics are strongly related. This notion is considered here within the framework of modified classical theory as represented by Eq. 14. This treatment of nucleation is classical in that Eq. 2, which is strictly thermodynamic in origin, provides for the basic arguments. Equation 14 contains the means of introducing growth kinetics into the nucleation mechanism; this is the feature exploited here that differs from Nielsen's treatment.

In most respects the results sought should be obtainable by the approach of Chiang et al. (1988). The approach employed by Narsimhan and Ruckenstein (1989) applies for Brownian motion kinetics and to nondissociating systems; a pertinent note is made below.

The growth kinetics considered eligible for consideration are obtained from the work of Chiang et al. (1988) and Nielsen (1969) as well as observations noted above. These are listed in the following three equations for crystals which are greater than critical size so that the Kelvin effect is not included. An expression which estimates diffusion-controlled growth rate is

$$(dr/dt) = Dv(c - c_e)/r. \quad (16)$$

Growth through surface diffusion of monomers to growth steps (BCF) or expressed as an empirical power law model is

$$(dr/dt) = k_g(c - c_e)^p, p \geq 1. \quad (17)$$

Chiang et al. (1988) provide, for sparingly soluble salt systems, the second-order expression based on a surface reaction (between ions) and subsequent integration into the crystal structure

$$(dr/dt) = k_{g2}(c^2 - c_e^2). \quad (18)$$

Nielsen also considered mononuclear and polynuclear mechanisms whose rate expressions are not included here. These are also discussed elsewhere (e.g., Ohara and Reid, 1973). Nielsen's development, which includes the above growth expressions and material balance considerations, is discussed in the appendix.

To reflect growth behavior of entities of near critical size, the Kelvin effect is included, and Eq. 17 becomes

$$(dr/dt) = k_g(c - c_e \exp[\Gamma/r])^p \quad (19)$$

and as implied by Eq. 18, for m -order kinetics

$$(dr/dt) = k_{gm}(c^m - c_e^m \exp[m\Gamma/r]). \quad (20)$$

Discussion of further justification of this step is provided by Chiang et al. (1988). It may be argued convincingly that the diffusion growth mechanism is not suitable for inclusion in Eq. 14 (Chiang et al., 1988). However, an equivalent expression appears to be implicit in the strictly Brownian motion arguments given by Narsimhan and Ruckenstein (1989) for nondissociating amorphous spherical systems. [This result may be obtained by a combination of equations in Narsimhan and Ruckenstein (1989, Eqs. 34, 36, 37, 39 and 44). It is restricted to large nuclei- $n^* \gg 1$.]

$$(dr/dt) = (Dv/r)(c_o - c_e \exp[r^* \ln S/r]) \quad (21)$$

Application to Experiments

From the resulting expression for N , Eq. 14A, one obtains

$$\ln N = \ln P - Q\beta\sigma^3 v^2 / (kT)^3 (\ln S)^2 \quad (22)$$

so that a straight line on $\log N - (\log S)^{-2}$ coordinates should result. The constant Q depends on the model used to describe growth after the immediate period of nucleation: $Q = 3/5$ for diffusion-controlled growth, $Q = 3/4$ for size-independent growth.

For the several growth expressions noted above and for the single growth model describing both nucleation and subsequent growth, the antilog of the intercept is described by the following:

Nielsen's model as described in Eq. 10A

$$P = 0.426 F_o v^{-6/5} (c_o - c_e)^{-1/5} \quad (23)$$

BCF surface diffusion or equivalent model, $p = 1$,

$$P = 2^{3/4} (3/\pi)^{1/4} N_o^{3/4} C_o^{1/4} \alpha^{3/4} F_G [c_o / (c_o - c_e)]^{1/2} \quad (24)$$

When $p > 0$, N is zero on applying L'Hospital's rule, the model is not eligible. Generally

For m th-order kinetics

$$P = [2m(3/\pi)^{1/3}]^{3/4} N_o^{3/4} C_o^{1/4} \alpha^{3/4} \cdot F_G (c_o^{m-1/3} (c_o - c_e)^{1/3} / (c_o^m - c_e^m))^{3/4} \quad (25)$$

For Brownian (diffusion based) nucleation and diffusion controlled growth

$$P = (75/16\pi)^{1/5} N_o^{3/5} C_o^{2/5} F_o \alpha^{3/5} [c_o / (c_o - c_e)]^{1/5} \quad (26)$$

In the above equations, $\alpha = [(n^*v)^{2/3} \sigma / kT]^{1/2}$. The mechanisms referred to in Eq. 26 are not the same as Nielsen's, as shown in Eq. 23. He obtained a $\log P$ value of 22.5. His development of the preexponential factor was explicit in its dependence on Brownian motion.

When diffusion-controlled growth occurs after the nucleation event by m th-order growth kinetics, $Q = 3/5$ and

$$P = (15/8\pi)^{2/5} m^{3/5} N_o^{3/5} C_o^{2/5} \alpha^{3/5} F_o \Theta^{-3/5} [c_o / (c_o - c_e)]^{1/5} \quad (27)$$

Because two growth mechanisms are implied in this expression, their kinetic parameters do not divide out. Rather, they appear explicitly in the dimensionless grouping Θ which reflects the ratio of controlling conductances at the moment of nucleation to that of subsequent growth. Similarly when Brownian based nucleation occurs followed by m th-order growth, $Q = 3/4$, and

$$P = 2^{5/4} N_o^{3/4} C_o^{1/4} \alpha^{3/4} F_G \Theta^{3/4} \cdot [c_o^{m-1/3} (c_o - c_e)^{1/3} / (c_o^m - c_e^m)]^{3/4} \quad (28)$$

In the above equations, $\Theta = Dc_o v / k_{gm} c_o^m (n^*v)^{1/3}$.

The sensitivity of P to growth kinetics, when nucleation is considered to depend only on Brownian contacts, is represented by the equations of Nielsen as given by Walton (1967)

$$N = 10^{22.2} \exp [(-3/5)(\Delta G^* / kT)]$$

$$N = 10^{22.7} \exp [(-4/3)(\Delta G^* / kT)]$$

$$N = 10^{22.4} \exp [(-3/4)(\Delta G^* / kT)]$$

for diffusion-controlled, mononuclear-controlled and polynuclear-controlled growth, respectively. Also of interest is that all three of the above mechanisms are not considered eligible here for consideration in the nucleation process. The first was discussed

immediately above; the latter two are difficult to model when the Kelvin effect exists.

Discussion

Data obtained for several systems by Nielsen (1967) and others (Mohanty et al., 1988; Bhandarkar et al., 1989; Makhija, 1988) are presented graphically in Figure 2. The wide spread of values for the intercept $\log P$ for these systems are listed in Table 1. The theoretical limit to $\log P$ is about 22.5 which is the approximate molecular density of the solid phases. The intercepts may be classified into two groups: those with greater values ($\log P > 27$) such as BaSO_4 , CaWO_4 , BaCrO_4 , and BaMoO_4 ; and those with smaller values ($\log P < 21$) such as PbSO_4 , PbCO_3 , BaCO_3 , Ca(OH)_2 , and Mg(OH)_2 . With the exception of sulfates, it appears that the classification is based on the type of anion; the double metal salts are included in the first group and carbonates and hydroxides, in the second. The higher intercept systems also show higher values for α , as determined from the slopes and discussed below.

The gypsum ($\text{CaSO}_4 \cdot 2\text{H}_2\text{O}$) system appears to be one for which several mechanisms may be competing: homogeneous, heterogeneous, and secondary (Makhija, 1988). Therefore, it is not considered to belong to either of the two categories identified above. It may indicate that systems exist which do not exhibit spontaneous nucleation (e.g., Table 3.1 in Nývlt et al., 1985).

Table 1 presents the values of $\log P$ as obtained from the appropriate expressions above and those determined from the experimental data shown in Figure 2. The supersaturations shown were obtained directly from c_0/c_e , i.e., $S_0 = S_c$. S may also be expressed in terms of activities, S_a , where $S_a = [(a_{\text{anion}}^x \times a_{\text{cation}}^y)/K_{\text{SP}}]^{1/(x+y)}$. For example, in the cases of Ca(OH)_2 and Mg(OH)_2 , the ionic activities can be calculated as described by Klein and Smith (1968) and by Klein et al. (1967) and an accounting for complex formation, e.g., $a_{\text{Ca(OH)}^+}$ and $a_{\text{Mg(OH)}^+}$, is taken into consideration. It is found that straight line extrapolation of the data so treated, $\log N$ vs. $(\log S_a)^{-2}$ yields the same intercept value as does the line graphed on $\log N$ vs. $(\log S_c)^{-2}$ coordinates. This is a consequence of the behavior $\lim_{c_0 \rightarrow \infty} c_0 \rightarrow \infty$, $(\log S_c)^{-2} = (\log S_a)^{-2} = 0$. The implied insensitiv-

ity of P to the method of expressing supersaturation supports P for use as a meaningful parameter. This assumes, of course, that the above methods for expressing S have some mechanistic validity. Chiang and Donohue (1988a) noted that actually supersaturation enters the formulation in a more indirect way for complex systems.

The extrapolation of the line (Figure 2) for high intercept systems gives a value for P which has no reality if one considers that the physical limit to N , number of nuclei/cm³, is imposed by the solid density ($\approx 10^{22.5}$ molecules/cm³). However, the data may be revealing through the slope of the lines graphed through them. According to the expressions derived above, the slope is related to the group

$$\alpha_1 = (\sigma v^{2/3}/kT)^{1/2}$$

by

$$\text{slope} = Q\beta\alpha_1^6/2.303^3$$

where $Q = 3/4$ or $3/5$ and β , the shape factor, has been taken to be $16\pi/3$ as representative of spherical form. The parameter α_1 , may be determined from the slope using the above relation. Knowing α_1 , it becomes possible to calculate the supersaturation S_0 at which n^* equals unity from

$$n^* = 2\beta\alpha_1^6/(\ln S)^3$$

Assumptions made in the theory do not permit consideration of such small values for n^* . However, it is considered here that this S_0 approximates the spinodal decomposition point. Recent discussions in the literature have included the notion of the spinodal in condensed solution systems (Myerson and Senol, 1984; Sorell and Myerson, 1986; Rasmussen, 1982). The values of c_0 at $n^* = 1$, listed in Table 1, were obtained solely from knowing α_1 . These values are seen to be less than the molecular density in solid phases for materials of the second classification (small α) and larger for the first (larger α). If one did venture to reason along these lines, a concluding suggestion is that if the mixing of still greater concentrations of reactants is performed rapidly enough, a spinodal effect would be involved in the phase change mechanisms for high α_1 systems.

Analysis of the Intercept

Nielsen's original equations describing the nucleation phenomenon took note that the first appearance of a new phase involves the two steps: nucleation *per se* and the growth of nuclei which accounts for the supersaturation decrease. The latter is of importance as it accounts for the termination of new particulate formation. Nielsen's derivations were modified to include nucleation which was not determined by the kinetics of Brownian motion. Termination of nucleation is significant, because it accounts for the total number of nuclei N which is determined experimentally. Nielsen also estimated t_1 for comparison with measured t_i . This experimental aspect of his work is not discussed here even though it serves as an indicator of the dynamics of the process. Measurement of the nucleation period t_i is useful for only some systems which yield fast growing nuclei so that counting of particles using the optical microscope is possible. Determination of N does not directly give dynamics information as it is meaningful only at $t \rightarrow \infty$. $N(S_0)$ does

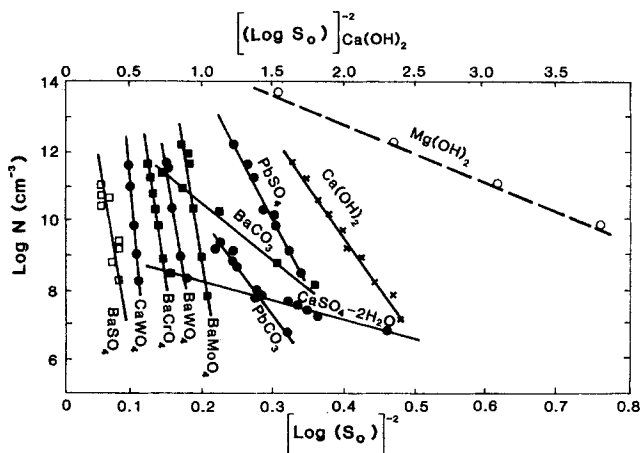


Figure 2. Experimental data for various systems using homogeneous nucleation.

The data are from: Mohanty et al. (1988) for BaSO_4 ; Bhandarkar et al. (1989) for Ca(OH)_2 and Mg(OH)_2 ; Makhija (1988) for $\text{CaSO}_4 \cdot 2\text{H}_2\text{O}$; and Nielsen (1967) for all others.

Table 1. Parameters Derived from Experimental Data and Modeled Log P Values: Nielsen log P value for Brownian nucleation, diffusion growth ~22.5

| Aqueous Systems | α_1^* | molecules/cm ³ | | | Log P | | | |
|---------------------|--------------|---------------------------|--------------------|----------------------|-------|-----------|-----------|------|
| | | c_e | c_o^{**} | $(c_o)_{n^*=1}$ | Exp. | A/B | C/D | E |
| BaSO ₄ | 2.45 | 6.0×10^{15} | 2×10^{19} | 1.5×10^{24} | 29.1 | 19.7/18.8 | 18.1/20.7 | 24.8 |
| CaWO ₄ | 2.42 | 1.4×10^{16} | 2×10^{19} | 2.1×10^{24} | 29.9 | 19.7/18.7 | | |
| BaCrO ₄ | 2.25 | 9.6×10^{15} | 3×10^{19} | 1.2×10^{23} | 27.4 | 19.9/19.0 | | |
| BaWO ₄ | 2.26 | 1.5×10^{16} | 3×10^{19} | 2.2×10^{23} | 29.9 | 19.9/19.0 | | |
| BaMoO ₄ | 2.24 | 1.2×10^{17} | 2×10^{19} | 1.3×10^{24} | 32.4 | 19.6/18.5 | | |
| PbCO ₃ | 1.75 | 2.4×10^{17} | 7×10^{18} | 4.6×10^{21} | 15.5 | 19.1/18.1 | | |
| BaCO ₃ | 1.63 | 6.0×10^{16} | 2×10^{19} | 3.0×10^{20} | 13.7 | 19.7/19.0 | | |
| PbSO ₄ | 1.83 | 7.8×10^{16} | 6×10^{19} | 3.7×10^{21} | 20.6 | 20.2/19.4 | | |
| Ca(OH) ₂ | 1.34 | 1.3×10^{19} | 9×10^{19} | 4.1×10^{21} | 19.7 | 20.1/19.1 | | |
| Mg(OH) ₂ | 1.09 | 9.0×10^{16} | 5×10^{19} | 4.2×10^{18} | 16.0 | 20.1/19.7 | | |

A = first-(BCF), second- or third-order kinetic model

B = Brownian nucleation kinetics and diffusion-controlled growth

C = reaction kinetics for nucleation- and diffusion-controlled growth

D = Brownian nucleation kinetics and reaction kinetics for growth

E = Nielsen's Brownian nucleation kinetics and reaction kinetics for growth

*Values calculated using $\beta = 16\pi/3$ for a sphere, and $Q = 1/2$

** c_o values obtained for log N = 10; within the experimental range for all systems except PbCO₃

suggest information concerning possible kinetics mechanisms through modeling arguments which are attempted here. We have taken Nielsen's modeling procedure to be fully applicable.

While developing Eq. 14 it was found that the nucleation mechanism depends on the group $[(dr/dt)/(d\Delta G/dr)]^*$. As suggested in the earlier development, both growth (dr/dt) and $d\Delta G(r)/dr$ necessarily approach zero as $r \rightarrow r^*$. This growth character may be modeled when the Kelvin effect pertains and reversible kinetics are applicable (Chiang et al., 1988). When the driving force for growth is described by a function which behaves as $[c - c_e \exp(\Gamma/r)]^p$, $p > 1$, nucleation as envisaged above does not occur.

The small intercept systems (Figure 2) may be accounted for using models for nucleation and crystal growth that are based on the same mechanism. Equations 23–26 represent these cases and Table 1 shows values for log P obtained from these models using $N_o = c_o$. These models seem to explain the small intercept systems inasmuch as the maximum values of log P obtained from these models (i.e., when $N_o = c_o$) are more nearly in the range and greater than the values derived from the data. The unknown parameter N_o provides for variability due to its uncertainty and may partially account for the deviations in the values of log P noted.

It may be noted that the exception to this observation is the system PbSO₄ whose experimental log P (or the intercept) is about equal to the maximum value of log P from theory. In that sense, PbSO₄ could be considered as an extreme example of the systems in the high intercept category. This is not surprising as the deviation may be attributed to the cation Pb which is of different chemical behavior from the alkaline earth cations of the other systems.

The smallest experimental intercept values [Table 1, PbCO₃, BaCO₃, Mg(OH)₂; and Figure 2, CaSO₄ · 2H₂O] may similarly be explained. That is, a Θ parameter may suggest two mechanisms for which the nucleation kinetic parameters are smaller than the growth parameters; or the roles of diffusion control and integration kinetics control are reversed so that Θ , as defined here, appears with a negative exponent, as in Eq. 27.

Equations 24–28 take the form

$$P = N_o^{3/4} C_o^{1/4} \Theta^{3/4}$$

or

$$P = N_o^{3/5} C_o^{2/5} \Theta^{-3/5}$$

when the grouping involving the numerical coefficient, F_o , F_g , α and the function involving the concentrations is taken to be unity. In the cases discussed here, this grouping is of order unity. When $\Theta = 1$, monomer incorporation mechanisms for nucleation ($r \leq r^*$) and growth ($r > r^*$) are the same. These cases are discussed in the preceding paragraph. When they are not the same, $\Theta > 1$. The expression for Θ given above, viz., $[(Dc_o v)/k_{gm} c_o^n (n^* v)^{1/3}]$ represents the ratio of Brownian or diffusion kinetics to reaction-type kinetics. That $\Theta > 1$ implies that Brownian kinetics represent the largest kinetics value independent of whether or not it is involved in nucleation or growth for the process under consideration. The magnitudes and variability of P are due to instantaneous initial concentration c_o and Θ . The surface energy parameter α , is influential indirectly through its presence in the exponent, and it seems to be an indicator of the different mechanisms implied in Θ . That is, $\Theta > 1$ when larger values of α_1 (and σ) are involved, suggesting that for large surface energy systems a transition in the mechanism of monomer addition occurs in passing from below to above the critical size.

Implied is that the mechanism of growth changes abruptly when the entity size achieves values greater than r^* . This is a complicated step in the phase change process that is actually in accord with the Nielsen's model in which growth mechanisms may differ from the Brownian mechanism for nucleation, and it may be accommodated in the models of Chiang et al. It is not too far fetched that once the size-supersaturation levels are such that the Kelvin effect is not involved, irreversibilities are introduced which cause a change in growth mechanism. The transition in growth mechanisms would have to be describable as a function continuous in the running variable r for the earlier descriptions to be strictly valid. In the cases shown in Table 1, the kinetic parameters involved included the diffusion coefficient (10^{-5} cm²/s) and k_{g2} [$4(\text{mol/L})^{-2} \cdot (\text{cm/s})$] for BaSO₄ (Chiang et al., 1988).

The magnitudes of average c_o values at which nucleation experiments are performed seem to be constant for all systems at

about 10^{19} molecules/cm³. This is consistent with the imposed constancy of B . For cases A and B, representative of one mechanism processes, the models suggest, as noted above, with $N_o = c_o$

$$P = c_o^{3/4}(c_o/n^*)^{1/4} \sim 10^{19}$$

$$P = c_o^{3/5}(c_o/n^*)^{2/5} \sim 10^{19}$$

with n^* averaging about 10. The n^* corresponding to the c_o varies with the system from about 3 and 4 (for BaCO₃, PbSO₄) to 32 (for BaMoO₄) with Mg(OH)₂ giving $n^* < 1$. These lower values suggest difficulties a. in obtaining experimentally-based slopes (or α_1) or b. weaknesses in the theory. A different procedure was involved in acquiring slopes for the Mg(OH)₂ system (Bhandarkar et al., 1989). The weakness in applied theory lies in the general structure of Nielsen's development, e.g., in the determination of $t_1(c_o)$. The classical theory, as employed here, is not rigorously applicable for such small values of n^* , e.g., as employed in the derivation of Eq. 14. Narsimhan and Ruckenstein's work (1989) makes this clear.

From Table 1, because log P magnitudes >22 , it is likely that $\Theta > 1$ for the first five systems listed. The increase exhibited over the single mechanism value 19 depends on the expression used for describing Brownian effects, either Nielsen's expression represented in the preexponential in Eq. 15 and employed in obtaining Eq. 23, or Eq. 21 and employed in obtaining Eq. 26. The former represents the classical preexponential with a value of about 32 and more nearly implies agreement with the experimental values, e.g., of 29 for the BaSO₄ system intercept.

If we continue to assume that Nielsen's development for determining the intercept value is sound, the suggestion implied above is that Brownian effects, as we have described them, are not represented adequately. The results of Narsimhan and Ruckenstein (1989) regarding Brownian kinetics is of interest here. They obtained results for the type system we consider here (their Figure 8) and show that nucleation results could in fact be orders of magnitude higher than classical predictions when spherical amorphous clusters are assumed to have been generated. Although we may have overextended elaboration of the Nielsen development here, this observation is of interest as it may lead to useful extension of this type of experiment and to further justifying the theoretical development.

The results of this analysis yield expressions for the y-axis intercept which are functions of the independent variable c_o . The intercept value corresponds to $c_o \rightarrow \infty$. The magnitude of c_o referred to represents a typical experimental value. This value turns out to be about 10^{19} for all systems considered except PbCO₃. That is, the experimental conditions which give a linear graphical presentation of the data (Figure 2) are represented by this value of c_o . Further, operation under these conditions (of c_o) are related to the experimental method employed. This condition yields nuclei numbers N in the range 10^7 – 10^{13} entities per milliliter. Operating at lower values yields results which are influenced by heterogeneous nucleation. Attempting operation with greater values leads to counting difficulties (Mohanty et al., 1988), operational difficulties such as mixing chamber plugging (CaSO₄ · 2H₂O), or results influenced by other mechanisms such as inadequate mixing, ripening, strictly chemical reaction effects (hydration and complex formation), or agglomeration. Successful operation effecting homogeneous nucleation outside

of the c_o range described above would be expected to show nonlinearity in the graphical presentation of Figure 2.

This discussion and the observation that $P \sim N_o(\text{max}) \sim c_o$ when the basic mechanisms of nucleation and growth are the same are significant. A spatially average consideration permits visualizing a shell of the solvent surrounding each solute nucleus; the ratio of their radii may be estimated as

$$[(1/c_o)/(n^*v)]^{1/3} \sim (10^{-19}/[10 \times 10^{-22.5}])^{1/3} \sim 10$$

This is the borderline distance at which nuclei show growth characters which are independent of each other (Nielsen, 1964, p. 30). That is, the concentration fields, in the case of diffusion-based growth, would not interfere with each other. This supports the general conclusion arrived at previously when similar mechanisms for nucleation and subsequent growth are involved, $\Theta = 1$.

Conclusions

This discussion suggests a basis for the existence of the wide range of experimental log P values that occur in the presentation of homogeneous nucleation results on log N vs. $(\log S_o)^{-2}$ coordinates. These values can be classified into two groups, one containing log P values >25 and the other, <21 . The combined nucleation-growth approach shows that the value of P is governed chiefly by N_o , c_o , and, with likelihood, a dimensionless ratio of the nucleation to growth kinetics parameters, Θ . For $\Theta = 1$ (growth and nucleation mechanisms for monomer addition are the same) and N_o set at its maximum value, c_o , what was developed here yielded log P values, which are about the same as some c_o obtained experimentally, viz., $18 < \log P < 20$.

Assuming full applicability of Nielsen's modeling procedure, deviations in the P value seem to lie with uncertainties in the density function coefficient, N_o and Θ . The larger experimental log P values require $\Theta \gg 1$ and classical Brownian nucleation best applies. Similarly the lower values of log P determined from the data could be explained by $\Theta < 1$, where Θ is appropriately defined so that the nucleation kinetics parameter value is less than that for growth kinetics. The significance of this is an implied change in the kinetics of monomer addition in going from below to above critical size.

Another characteristic of the two categories is the parallel behavior of α_1 values, which are obtained from the slopes of the lines seen in Figure 2. Greater α_1 values suggest a change in mechanisms of monomer addition during and beyond the formation of a critical nucleus; in Table 1, first five systems, the likely nucleation mechanism is described using classical Brownian kinetics. For growth mechanisms which are of a higher order in $(c_o - c_e)$, e.g., as indicated by $p > 1$ in Eqs. 17 and 24, either no nucleation occurs or heterogeneous nucleation is the initiating mechanism. This explanation may include the precipitation behavior of hydrated systems (such as CaSO₄ · 2H₂O in Figure 2) and more generally low σ value (high-solubility) systems.

Acknowledgment

We acknowledge the support provided for this work by the NSF Grant No. CBT8502409.

Notation

a = activity of the solute in solution
 A = surface area of an embryo

c = instantaneous molecular concentration of the solute
 c_e = equilibrium molecular concentration or solubility of the solute
 c_o = initial molecular concentration before onset of reaction
 C_o = apparent embryo concentration, c_o/n^*
 D = diffusion coefficient of the monomeric specie
 D_n = so-called diffusion coefficient, required to satisfy Eq. 6 and assumed correct as given in Eq. 8
 D_r = same as D_n but considered as a function of r , instead of n
 f_n = distribution function of the embryo sizes
 F = correction factor required in Eqs. 9A and 11A with appropriate subscripts, F_o and F_G
 G = Gibbs free energy of the new phase
 G_o = linear growth rate (dr/dt) for concentration c_o
 J = instantaneous nucleation rate
 J_o = initial nucleation rate corresponding to c_o
 k = Boltzmann constant
 k_{gm} = rate constant for m th-order reaction
 n = number of monomers in an aggregate or cluster
 \dot{n} = increase rate of cluster size, monomers per unit time; equivalent linear growth rate written as (dr/dt)
 N = final number of nuclei
 p = order of the reaction common for nucleation and growth
 P = intercept value of the line on $\log N$ vs. $(\log S_o)^{-2}$ coordinates, N at $S_o \rightarrow \infty$
 Q = factor in the expression for P due to the type of growth, cf. Eqs. 15A and 22
 r = radius of an embryo
 S = instantaneous supersaturation ratio, c/c_e
 S_o = initial supersaturation ratio, c_o/c_e
 t = time
 t_i = induction period, experimentally measured time for appearance of turbidity
 t_m = mixing time scale, calculated time for completion of mixing of the two reactants
 t_n = time scale for reaching the steady-state distribution of embryos
 t_1 = time scale for nucleation, calculated through Nielsen's procedure of derivation
 T = temperature
 v = volume of the monomeric specie
 V = volume of the embryo

Greek letters

α = dimensionless group $[\sigma(vn^*)^{2/3}/kT]^{1/2}$; in accordance with Eq. 2, $(vn^*)^{2/3}$ implies the area per embryo or cluster
 α_1 = supersaturation independent grouping in α , $(v^{2/3}\sigma/kT)^{1/2}$
 β = shape factor, $4A^3/27V^2$
 Θ = dimensionless group, $[Dv/k_{gm} c_o^{m-1}(n^*v)^{1/3}]$; in accordance with Eqs. 16 and 18, this group implies the ratio of diffusion transfer kinetics to integration reaction kinetics
 σ = interfacial tension associated with new phase
 τ = running time variable for one nucleus, $\tau = 0$ at moment of nucleation

Literature Cited

- Bhandarkar, S., R. Brown, and J. Estrin, "Studies in Rapid Precipitation of Hydroxides of Calcium and Magnesium," *J. Crystal Growth*, **97**, 407 (1989).
 Chiang, P., and M. D. Donohue, "The Effect of Complex Ions on Crystal Nucleation and Growth," *J. Coll. Int. Sci.*, **126**, 579 (1988b).
 ———, "A Kinetic Approach to Crystallization From Ionic Solution: Crystal Growth," *J. Coll. Int. Sci.*, **122**, 230 (1988a).
 Chiang, P., M. D. Donohue, and J. L. Katz, "A Kinetic Approach to Crystallization From Ionic Solution: Crystal Nucleation," *J. Coll. Int. Sci.*, **122**, 251 (1988).
 Frenkel, J., *Kinetic Theory of Liquids*, Dover, New York (1955).
 Kagan, Y., "The Kinetics of Boiling of a Pure Liquid," *Russian J. Phys. Chem.*, **34**, 42 (1960).
 Katz, J., "Condensation of a Supersaturated Vapor. I. The Homogeneous Nucleation of the n -Alkanes," *J. Chem. Phys.*, **52**, 4733 (1970).
 Katz, J., and M. D. Donohue, "A Kinetic Approach to Homogeneous Nucleation Theory," *Adv. Chem. Phys.*, **40**, 137 (1979).
 Klein, D. H., and M. D. Smith, "Homogeneous Nucleation of Calcium Hydroxide," *Talanta*, **15**, 229 (1968).

- Klein, D. H., M. D. Smith, and J. A. Driy, "Homogeneous Nucleation of Magnesium Hydroxide," *Talanta*, **14**, 937 (1967).
 Lothe, J., and G. M. Pound, "Reconsiderations of the Nucleation Theory," *J. Chem. Phys.*, **36**, 2080 (1962).
 Makhija, S., M. S. Thesis, "The Influence of Nucleation in the Setting of Gypsum Plaster," Univ. of Rhode Island (1988).
 Mohanty, R., S. Bhandarkar, B. Zuromski, R. Brown, and J. Estrin, "Characterizing the Product Crystals from a Mixing Tee Process," *AIChE J.*, **34**, 2063 (1988).
 Myerson, A. S., and D. Senol, "Diffusion Coefficients Near the Spinodal Curve," *AIChE J.*, **30**, 1004 (1984).
 Nielsen, A. E., *Kinetics of Precipitation*, Pergamon Press, Oxford (1964).
 ———, "Nucleation in Aqueous Solutions," *Crystal Growth*, H. S. Peiser, ed., Pergamon Press, Oxford (1967).
 ———, "Nucleation and Growth of Crystals at High Supersaturations," *Kristall und Technik*, **4**, 17 (1969).
 Nielsen, A. E., and O. Sohnel, "Interfacial Tensions Electrolyte Crystal-Aqueous Solution from Nucleation Data," *J. Crystal Growth*, **11**, 233 (1971).
 Narsimhan, G., and E. Ruckenstein, "A New Approach for the Prediction of the Rate of Nucleation in Liquids," *J. Coll. Int. Sci.*, **128**, 549 (1989).
 Nyvlt, J., O. Sohnel, M. Matuchova, and M. Broul, *The Kinetics of Industrial Crystallization*, Elsevier (1985).
 Ohara, M., and R. C. Reid, *Modeling Crystal Growth Rates from Solution*, Prentice-Hall (1973).
 Rasmussen, D. H., "Energetics of Homogeneous Nucleation-Approach to Physical Spinodal," *J. Crystal Growth*, **56**, 45 (1982).
 Schmitt, J., "A Study of Vapor Phase Self-Initiated Thermal Polymerization of Styrene with an Expansion Chamber," *J. Chem. Phys.*, **89**, 5307 (1988).
 Sorell, L. S., and A. S. Myerson, "The Diffusivity of Urea in Concentrated Saturated and Supersaturated Solutions," *AIChE J.*, **28**, 772 (1982).
 Strickland-Constable, R. F., *Kinetics and Mechanism of Crystallization*, Academic Press, London (1968).
 Walton, A. G., *The Formation and Properties of Precipitates*, Interscience, New York (1967).
 Wegener, P. P., "Nonequilibrium Flow with Condensation," *Acta Mech.*, **21**, 65 (1975).
 Zeldovich, J. B., "On the Theory of New Phase Formation: Cavitation," *Acta Physicochimica U.R.S.S.*, Vol. XVIII, No. 1, 1 (1943).

Appendix

Nielsen's development of the expressions for N follows. Equation 14 takes the general form

$$J = B \exp [-\Delta G^*/kT] \quad (1A)$$

where B is dependent only weakly on the supersaturation S compared to the exponential factor. As a consequence,

$$d \ln J / d \ln c \approx 2\beta\sigma^3 v^2 / (kT \ln S)^3 = n^*. \quad (2A)$$

Taking n^* to be constant the nucleation rate as a function of c may be estimated

$$J = J_o (c/c_o)^{n^*} \quad (3A)$$

Nielsen (1969) points out that the assumption of constant n^* is good for most systems and for a large range of initial concentrations c_o . J_o is the rate of nucleation corresponding to $c = c_o$. If all nuclei have been generated by the time $t = t_1$, then Eq. 1 may be rewritten to include the above approximation

$$N = \int_0^{t_1} J dt = J_o \int_0^{t_1} (c/c_o)^{n^*} dt \quad (4A)$$

The remaining consideration is that of determining t_1 , the period during which most nucleation occurs. For material balance considerations, Nielsen assumed that the influence of the Kelvin effect occurs over an insignificantly small part of the period t_1 for most nuclei and need not be considered. Thus for diffusion-controlled growth Eq. 16 is applicable and $c(t)$ may be obtained from

$$v[c_o - c(t)] = (4\pi/3) (2Dv)^{3/2} \cdot \int_0^t \left[\int_\tau^t (c - c_e) dt' \right]^{3/2} J(c) d\tau \quad (5A)$$

As nucleation is very sensitive to c in contrast to growth, a solution to the above, valid as an estimation for small time, may be obtained by replacing J by J_o and $(c - c_e)$ by $(c_o - c_e)$. Equation 5A then gives

$$c = c_o - (8/15)\pi(2D)^{3/2} v^{1/2} J_o(c_o - c_e)^{3/2} t^{5/2} \quad (6A)$$

This provides an estimate for t_1 , i.e., at $t = t_1$, $c = c_e$ and the above yield

$$t_1 = (15/16 \pi \sqrt{2})^{2/5} \{D^{3/2} J_o [v(c_o - c_e)]^{1/2}\}^{-2/5} \quad (7A)$$

On combining Eqs. 5A and 6A, with some algebraic manipulation

$$(c - c_e) = (c_o - c_e) [1 - (t/t_1)^{5/2}] \quad (8A)$$

This may be inserted into the integrand of Eq. 4A to obtain

$$N = J_o t_1 F_o \quad (9A)$$

where

$$F_o = \gamma^{2/5} \int_0^\gamma (1 - y^{5/2})^{n^*} dy$$

and

$$\gamma = c_o/(c_o - c_e).$$

The parameter n^* has been assumed constant. In general the equations developed above are the same as Nielsen's except that the difference $(c_o - c_e)$ is involved above whereas Nielsen took $c_o \gg c_e$. On using Nielsen's expression for J_o , Eq. 15, and Eq. 7A

for t_1 , Eq. 9A becomes

$$N = 0.281 F_o / [v^{6/5} (c_o - c_e)^{1/5}] \cdot \exp [-3/5 (\Delta G^*/kT)] \quad (10A)$$

The factor $3/5$ originates from the material balance in which diffusion-controlled growth was assumed. Furthermore, the diffusion coefficient was employed in elucidating nucleation kinetics as well. The consequence is that this dynamic parameter divided out in obtaining the final expression for N . This result is as might be expected for N is not a dynamic quantity and represents a property of the system that is fully time-independent.

The same procedure may be applied to the case where growth is described by size-independent expressions before the Kelvin modification is employed; e.g., growth expressions such as Eq. 17 or 18 may apply. The development leads to an expression which serves to replace Eq. 9A

$$N = J_o t_1 F_G \quad (11A)$$

where

$$F_G = \gamma^{1/4} \int_0^{\gamma^{-1/4}} (1 - y^4)^{n^*} dy$$

and,

$$t_1 = [v(c_o - c_e)/G_o^3 J_o \pi/3]^{1/4} \quad (12A)$$

On combining the above and using Eq. 1A the expression for N becomes

$$N = F_G (B/k_g)^{3/4} \cdot [\pi(c_o - c_e)^{3p-1}/3v]^{-1/4} \exp [-3/4 (\Delta G^*/kT)] \quad (13A)$$

The preexponential factor B is derived from Eq. 14. On inspection of Eqs. 13A and 14 the dynamical parameter k_g will divide out if it is used in providing explicit elaboration of $(dr/dt)^*$ in the expression for B .

In general the expression for N may be represented as

$$N = P \exp [-Q\beta\sigma^3 v^2/(kT)^3 (\ln S)^2] \quad (14A)$$

as is evident when comparing Eqs. 10A and 13A. This leads to Eq. 22 in the text.

Manuscript received Dec. 27, 1989, and revision received Aug. 7, 1990.